

Gait Verification System for Criminal Investigation

HARUYUKI IWAMA^{1,a)} DAIGO MURAMATSU^{1,b)} YASUSHI MAKIHARA^{1,c)} YASUSHI YAGI^{1,d)}

Received: March 27, 2013, Accepted: July 22, 2013, Released: October 18, 2013

Abstract: This paper describes the first gait verification system for criminal investigation using footages from surveillance cameras. The system is designed so that the criminal investigators as non-specialists on computer vision-based gait verification can, independently, use it to verify unknown perpetrators as suspects or ex-convicts in criminal investigations. Each step of the gait verification process is proceeded by interactive operation on a graphics-user interface. Eventually, for each pair of compared subjects selected by a user, the system outputs a posterior probability on a verification result, which indicates that compared subjects are the same, with the consideration of various circumstances of the subjects such as the size, frame-rate, observation views, and clothing of subjects. One gait-specialist and ten non-gait-specialists participated in operation tests of the system using five different datasets with various types of scenes, each of which contained two or three verification sets. It was shown that all the non-gait-specialists, as well as the gait-specialist, could obtain reasonable verification results for almost all of the verification sets.

Keywords: gait verification system, decision-support system, criminal investigation, biometrics

1. Introduction

Surveillance footage-based person verification techniques are beginning to play an important role in criminal investigation with the significant increase in the use of surveillance cameras. In particular, gait, as a behavioral biometric cue, has attracted much attention in recent years because of the difficulty in disguising it and the ability to discriminate subjects at a distance without requiring their cooperation. In fact, many gait recognition techniques have been developed [1], [2], [3], [4], [5] in the computer vision community. In addition, gait verification from closed-circuit television (CCTV) images has been admitted as criminal evidence against a burglar in UK courts [6], and gait evidence has also been used as a cue for criminal investigation in Japan.

One of the primary tasks of gait recognition from surveillance footages in criminal investigation [7] is to verify the unknown perpetrator (criminal person) as a suspect or someone with a criminal record in a quantitative way by analyzing the gait computationally. The point is that the verification result influences much on the strategic direction of criminal investigation, and furthermore, it could be judged as a criminal evidence at subsequent stage, court. Therefore, the verification result should have sufficient properness and validity. To obtain such verification result, the analyst (person in charge of verification) should make sure that the processed results in each step of gait verification (e.g., subject detection, tracking, segmentation, and feature extraction) contain no unintended errors.

From this point of view, it is preferable to obtain the verification

result by an interactive procedure composed of automatic and manual processes, so that any error in the results can be corrected by manual checking and judgment, rather than using fully automatic software^{*1}.

To complete such a procedure, specialist knowledge on computer-vision-based gait analysis is required, which most criminal investigators (e.g., police officers and intelligence agency) do not possess, because it is a relatively new area of study [8] and has not yet been in common use like fingerprint and face analysis. Moreover, there is no packaged software tool which carefully assists the task. Consequently, the criminal investigators need to hand the task to gait-specialists such as the computer vision researchers specializing in gait analysis^{*2}. An example of the work flow involved in gait verification is illustrated in Fig. 1.

While requesting help from gait-specialists is to some extent a reasonable solution, it is inefficient in time and cost for use in every criminal case. In particular, time is often crucial for the initial investigation. Therefore, it is desirable for criminal investigators to execute gait verification by themselves in a timely manner.

With this motivation, we have constructed a gait verification system as an analytical tool for criminal investigation to replace the work of the gait-specialist as shown in Fig. 1. The system is designed specifically for non-gait-specialists such as criminal investigators, so that they can obtain gait verification results by simply learning the system operation following the instruction manual. To the best of our knowledge, this system is the first gait verification system established for criminal investigation, except for unpublished private systems.

Although there are various scenarios for perpetrator verifica-

¹ The Institute of Industrial and Scientific Research, Osaka University, Osaka 567-0047, Japan

^{a)} iwama@am.sanken.osaka-u.ac.jp

^{b)} muramatsu@am.sanken.osaka-u.ac.jp

^{c)} makihara@am.sanken.osaka-u.ac.jp

^{d)} yagi@am.sanken.osaka-u.ac.jp

^{*1} There is no algorithm which can guarantee *perfect* results all the time.

^{*2} In fact, Japanese police have requested our laboratory gait verification services at least once a month over the last few years.

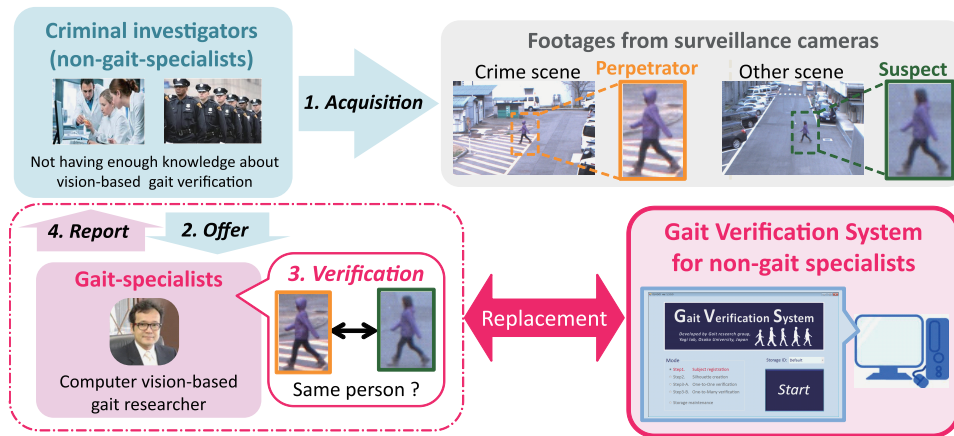


Fig. 1 An example of the work flow of gait verification and the aim of the constructed system. First, the criminal investigators acquire footages of a perpetrator and a suspect. They offer the gait verification task to a gait-specialist such as computer vision-based gait researcher, who then verifies the perpetrator against the suspect based on gait analysis. Finally, the gait-specialist reports the results to the criminal investigators, whose next action in the criminal investigation is based on these results. The replacement of the gait-specialist in this work flow is the purpose of the constructed system.

tion, we focus on the following two scenarios,

- (1) One-to-one verification: individualized verification against the specified suspects in other surveillance footages,
- (2) One-to-many verification: batch verification against people registered on the databases of criminal records in the criminal intelligence agency.

Note that one-to-many verification essentially covers one-to-one verification from a technical view point, that is, a one-to-many verification procedure is achieved by a batch process of one-to-one verification. We consider the two scenarios separately for convenience in practical applications.

The system provides two types of verification functions associated with the two scenarios and supports the whole process of gait verification, from subject selection to gait feature matching. The input and output of the constructed system are shown in **Fig. 2** and the key characteristics of the system are listed as follows.

- **Usability intended for the non-gait-specialist**

The system has a graphics-user interface (GUI) so that a user, who has no specialist knowledge of computer vision-based gait analysis but is computer literate, can proceed through each process of gait verification interactively. In addition, several automatic processing functions are implemented to reduce the burden of manual operation.

- **Professional gait analysis**

The Gait Energy Image (GEI) [1], which is the most widely used and has high discrimination capability [9], is used as the gait feature for verification. In addition, a view transformation model [2], [10] enables verification between subjects captured from different observation views.

- **Objective output**

The verification result is output in the form of the posterior probability of the distance score between compared gait features. In the one-to-one verification function, a pair of subjects (a probe subject and a gallery subject) is matched and a corresponding posterior probability is output. In the one-to-many verification, a probe subject is matched to all the

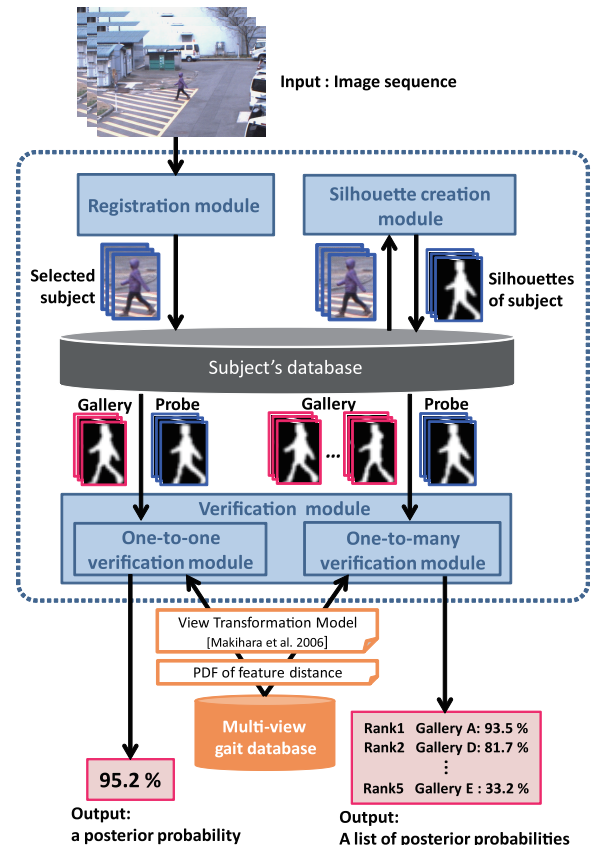


Fig. 2 Data flow of the constructed system.

gallery subjects in the system database, and a list of the candidates with the highest posterior probabilities is output in descending order. Note that the system simply outputs these objective values, and never makes any judgment.

- **Applicability to various circumstances**

The circumstances of the compared subjects are often different (e.g., image resolution, captured frame rate, observation view, clothing, and baggage). It is known that the performance of gait recognition is influenced by these cir-

cumstances [9], [11], [12]. Therefore, in order to compute a reliable posterior probability, it should be computed based on circumstance-dependent probability density functions (PDFs) of distance score. In the constructed system, the circumstance-dependent PDFs are arranged by means of multi-view gait dataset, and the system computes a circumstance-dependent posterior probability as an output.

A prime contribution of this work is that it is the first construction of a system as a packaged tool for gait verification in criminal investigation, and it is not a proposal for a novel gait verification algorithm in itself. Moreover, it should be noted that the system is simply a decision-support system for criminal investigators (non-gait-specialists), and is not a decision (judgment) making system.

In fact, this system is a major upgrade of the previously reported system [13] and the following extensions widen its range of applications.

- Cross-view verification based on the view transformation model [2], [10]: The previous version only supports the same-view verification (observation views of an input pair of subjects must be the same). On the other hand, the observation view of surveillance footage is varied on a crime by crime, and thus the observation views of an input pair of subjects are frequently different in general. As a result, the application range of the previous system is significantly limited in criminal investigation. Therefore, we introduce the view transformation model-based gait feature matching framework to realize the cross-view verification which extremely enhances the practical value of the system.
- One-to-many verification function: While we consider the two verification scenarios as described above, the previous system only supports the one-to-one verification function. From the view point of system usability, the one-to-many verification function as another independent function from one-to-one verification is preferable to be developed (e.g., it seems to be nonsense to use one-to-one verification function repetitively for one-to-many verification when dozens of pairs are verified at one time). Therefore, we added the one-to-many verification function as another module.

The outline of this paper is as follows. We summarize related work in Section 2, and describe the gait verification framework in Section 3. The details of the constructed system are then described in Section 4 and the effectiveness of the system is evaluated via operation tests carried out by eleven users in Section 5. The discussion is presented in Section 6. Finally, we give our conclusions in Section 7.

2. Related Work

2.1 Video-based Gait Analysis

Video-based gait analysis has been widely studied as an approach to acquiring soft biometrics such as age [14], [15] and gender [16] as well as hard biometrics, namely, the identification of a person using model-based approaches [17], [18], [19], [20] or appearance-based approaches [1], [2], [3], [4], [5], [21], [22].

Although model-based approaches have several advantages over appearance-based ones (e.g., view invariance) and there exist some model-based gait analysis services [23], [24], [25], these

often require good quality images to calculate model parameters with high accuracy from a gait sequence, which may be difficult to obtain from many surveillance cameras.

On the other hand, there has been a recent trend towards appearance-based approaches because of low computational cost and robustness to noise, and in general a tendency to outperform model-based approaches. Of the appearance-based approaches, Iwama et al. [9] reported that the GEI [1], also known as the averaged silhouette [21], achieved the best performance given the large population gait database [26]. In addition, Matovski et al. [27] reported that the GEI-based gait recognition performance was almost unchanged after a year long time lapse, indicating the real possibility of using gait as a tool for criminal investigation.

2.2 Biometric System for Criminal Investigation

The relationship or difference between biometrics and forensics is discussed in Refs. [28] and [29].

Many biometric modalities have been used in crime investigations. As early as 1881, Bertillon proposed to identify reoffenders based on anthropological methods [30]. In his method, 11 anthropometric characteristics were measured, and used together with a description of the iris color for identification.

Faulds proposed in 1880 the use of fingerprints for the purpose of investigative identification [31]. Around the same time, Herschel used fingerprints to identify individuals, and undertook a study on the permanence of the fingerprints [32]. After that Galton evaluated the permanence and uniqueness of fingerprints, and proposed classification methods for fingerprints at the end of the 19th century [33]. Henry proposed a fingerprint classification system [34]. Since then, fingerprints have been employed as useful marks of identity and in automated systems [35].

Nowadays, deoxyribonucleic acid (DNA) is frequently screened for at crime scenes for identification purposes [36] because DNA can be obtained from biological stains of blood samples, saliva, and hair follicles. Handwriting-based methods have also been proposed [37], [38], [39], because ransom letters or threatening letters associated with blackmail can include handwritten characters that can provide clues to identifying perpetrators. Ear [40], [41] and teeth or bitemarks [42], [43] are also useful in crime investigations.

Digital traces including recordings from phone-tapping and surveillance cameras are also available, and voice or speech [44], [45], [46], face [47], [48], [49], [50], and gait recognition [7], [51], [52] can be used in crime investigation analysis.

As mentioned above, many biometric modalities have been used for criminal investigation, and various systems for person verification in criminal investigation that use modalities including fingerprints, face, speech, handwriting, and ear are reported (e.g., [35], [38], [41], [53], [54]). To the best of our knowledge, no such verification system based on gait has been reported. Although a type of gait identification system [55] for visual surveillance has been developed, it is unsuitable for use in criminal investigation mainly because, (i) it does not support interactive functions such as the manual correction of errors in automatically processed results, (ii) it cannot be applied to the various circumstances of subjects (as listed in Section 1).

3. Gait Verification Framework

In this section, we describe a framework for gait verification between a pair of subjects (probe and gallery subjects), implemented in the constructed system. In the verification process, two subjects are compared using their gait features, and the result is represented as a posterior probability, which indicates the extent to which they could be the same subject.

3.1 Gait Feature

The GEI [1] is used as the gait feature, because it is the most widely used owing to its high discrimination performance as reported in Ref. [9]. The GEI is obtained by averaging silhouettes over a gait cycle and its process is illustrated in Fig. 3.

The GEI is created as following procedures. First, silhouette of a target subject is extracted as foreground in each frame of a given gait sequence. Next, registration and size-normalization are carried out for the extracted silhouette sequence. In this step, the height and horizontal center of the silhouette regions are obtained for each frame, and silhouette regions are scaled so that the height is just pre-defined size, while maintaining the aspect ratio (e.g., 88 by 128 pixels). Then, the gait period M is calculated based on the Normalized Auto Correlation (NAC) of the size-normalized silhouette sequence (see the work of Ref. [2] for further details about gait period estimation). Finally, a GEI is obtained by averaging size-normalized silhouettes over a gait period as,

$$GEI(x, y)_k = \frac{1}{M} \sum_{t=k}^{M+k} I(x, y, t), \quad (1)$$

where k is the first frame identifier in GEI calculation and $I(x, y, t)$ is the silhouette value (0: background, 1: foreground) at the position (x, y) at the t -th frame. The creation process is illustrated in Fig. 3.

3.2 Gait Feature Matching

For a given gait sequence composed of N frames in which the gait period is M frames ($M \leq N$), $N - M + 1$ different sections of the gait period can be found by shifting the initial frames, and we compute the GEI for each section. We then let L_p and L_g be the numbers of sections in the probe and gallery sequences and $\mathbf{x}_{p,k}$ and $\mathbf{x}_{g,k}$ are the GEIs of probe and gallery subjects at the k -th section, a feature distance D between probe and gallery subjects is defined as,

$$D = \min_{i,j} \|\mathbf{x}_{p,i} - \mathbf{x}_{g,j}\|_2, \quad (2)$$

where i ($1 \leq i \leq L_p$) and j ($1 \leq j \leq L_g$) are the section identifiers in the probe and gallery sequences, and $\|\cdot\|_2$ is the Euclidean distance.

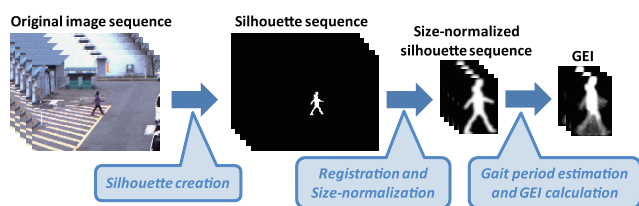


Fig. 3 GEI creation process.

3.2.1 View and Clothing-invariant Matching

When the circumstances of the compared subjects differ, the differences may affect the discrimination capability of the gait feature. In particular, the differences in the observation view and clothing (or baggage) seriously degrade the discrimination capability as reported in Refs. [11] and [56]. Furthermore, such differences might spoil the verification validity in essential.

Therefore, we incorporate view-invariant gait feature matching using a view transformation model [2] (VTM), which enables us to transform a gait feature with one view into that with another view. Figure 4 illustrates the VTM-based gait feature matching.

In this scheme, the VTMs are trained in advance for all the pairs of predefined discrete observation views by GEIs of non-target training subjects (e.g., volunteers such as lab. members) with the observation views in training stage. More specifically, view transformation (mapping) matrix $A(\theta_i, \theta_j)$ of gait feature from view θ_i to view θ_j is trained for all the combinations (θ_i, θ_j) .

In matching stage, an input pair of GEIs of target subjects (e.g., perpetrator and suspect) with different observation views is matched after view transformation by $A(\theta_i, \theta_j)$, in which one GEI is transformed so that its observation view becomes the same as that of the other GEI. In Fig. 4, for example, the gallery GEI \mathbf{x}_{g,θ_2} with observation view θ_2 is transformed by VTM (matrix) $A(\theta_2, \theta_k)$ to the GEI $\hat{\mathbf{x}}_{g,\theta_k} (= A(\theta_2, \theta_k)\mathbf{x}_{g,\theta_2})$ with observation view θ_k which is the observation view of probe GEI (see the work of Ref. [2] for further detail procedures).

Also, we introduce the concept of part-based gait feature matching [56] via spatial feature masking for clothing-invariant matching. An example of feature masked matching is illustrated in Fig. 6 (P) and (Q).

Putting it all together, the GEI \mathbf{x} used for the distance calculation is rewritten as \mathbf{x}' , which is the view-transformed and spatially masked GEI. Of course, for each of the compared subjects, specifications for the view and mask are needed. The detailed processes of such specifications in this system are described in

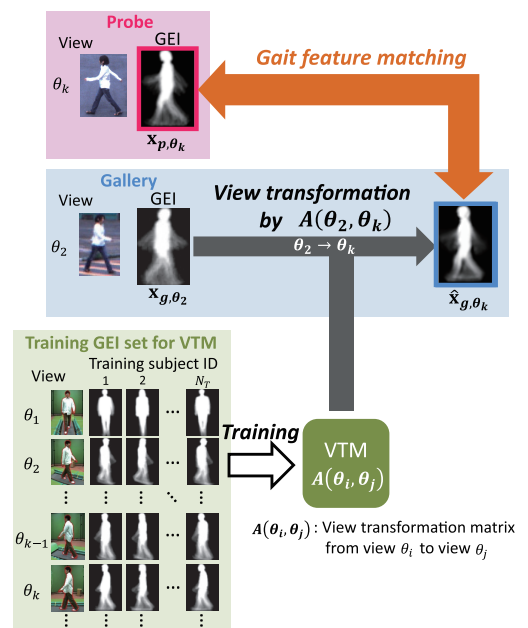


Fig. 4 VTM-based gait feature matching.

Table 1 Definition of factors.

Factor	Variations
Size of the GEI	22 by 32 [pixels] and 44 by 64 [pixels]
Frame rate	5, 7.5, 15, 30 [fps]
Observation view	12 azimuth views times 2 tilt angles (Fig. 9 shows the sample image from each angle)
Feature mask	11 by 16 [blocks] (as shown in Fig. 11 (a))

Section 4.

3.3 Circumstance-dependent Posterior Probability

After the calculation of a feature distance, the distance score is mapped to a posterior probability of the same person with consideration of the circumstances (e.g., camera setting, observation view, and clothing). Let I_p and I_g be information describing the circumstances of the probe and gallery subjects, and then a circumstance-dependent posterior probability for a given distance score D is calculated as:

$$P(X=1|D; I_p, I_g) = \frac{P(D|X=1; I_p, I_g)P(X=1)}{\sum_X P(D|X; I_p, I_g)P(X)}, \quad (3)$$

where X is a random variable which represents whether the compared subjects are the same ($X=1$) or different ($X=0$).

3.3.1 Definition of Circumstances

To calculate the posterior probability shown in Eq.(3), a circumstance-dependent probability density function (PDF) of the distance score in each class ($P(D|X; I_p, I_g)$, $X \in \{0, 1\}$) needs to be trained^{*3}. For example, let us focus on the observation view as a circumstance. If we discretely approximate the azimuth view at a relatively fine level, while the approximation error could be sufficiently small, it explosively increases the required number of PDFs to cover all the combinations of the probe and gallery views (e.g., 1 [deg] interval leads to 64,980 combinations ($_{360}C_2$ for cross view and 360 for the same view), which also means the explosive increase of the training gait features for the combinations. On the other hand, the combination number becomes smaller if we consider more coarsely-discretized observation views. In such a case, however, the approximation error becomes larger and the validity of posterior probability is degraded.

Therefore, the circumstance should be defined carefully and appropriately by considering the tradeoff between the validity of the calculated posterior probability and the availability of the training data.

Taking into account the above discussion, we focus on four factors, the size of the subject in the captured image, captured frame rate, observation view, and feature mask region, as information that describes the circumstances that affect the PDFs. For the size of the subject, we consider the normalized size of the subject's silhouette for GEI creation, that is, the (template) size of the GEI. In addition, we quantize the variation of each factor as shown in the **Table 1**. Note that we consider the feature mask as a block-wise mask as shown in Fig. 11 (a). Consequently, we define these factors as circumstances and calculate the factor-dependent PDFs as circumstance-dependent PDFs.

Note that these circumstances should be specified for each verified pair of subjects in the system. The details of these specifications in the system's operation are described in Section. 4.

3.4 Training of VTM and Circumstance-dependent PDF

3.4.1 Training Database

We used a multi-view gait database comprising two datasets^{*4}, one for training the VTMs and the other for training the circumstance-dependent PDFs. Both datasets were composed of sets of size-normalized silhouette sequences of normal walking on the treadmill captured by 24 cameras (12 azimuth views times 2 tilt angles), each of which corresponds to each observation view defined as the factor of circumstances. The normalized size was 88 by 128 pixels and the captured frame rate was 60 fps. The former dataset included 114 sequences of 82 subjects (one or two sequences per subject), and the latter included 206 sequences of 103 subjects (two sequences per subject).

We then generated additional silhouette sequences with different sizes (22 by 32 and 44 by 64 pixels) and different frame rates (5, 7.5, 15, and 30 fps) by resizing and resampling the original size-normalized silhouette sequences in both datasets, which were regarded as the extended datasets.

3.4.2 Training of VTM

By considering the sizes of the GEI and the frame rates, the VTMs about the GEI between all possible combinations of the observation views were trained using the extended dataset. Note that the trained VTMs were dependent on the frame rates, the sizes of the GEI, and observation views.

3.4.3 Training of Circumstance-dependent PDF

The distributions of distance scores for all combinations of the four factors were calculated using the extended dataset, in each of which two sequences were arranged for each subject, one as a gallery sequence and the other as a probe sequence. The distance score is calculated for each pair of gallery and probe sequences. The corresponding PDF is then estimated by non-parametric kernel density estimation using a Gaussian kernel.

4. Gait Verification System

4.1 Overview

The system is designed to be used as a tool for criminal investigators (non-gait-specialists), providing gait verification between probe and gallery subjects registered in the system from their input image sequences. Note that for descriptive purposes we consider the perpetrators as probe subjects and the suspects and those with previous convictions as gallery subjects in this system.

The system is composed of a subject database and four modules: registration, silhouette creation, one-to-one verification, and one-to-many verification modules. The data flow of the system

^{*3} Prior probabilities $P(X)$ are also set for calculating the posterior probability. We set neutral probabilities to $P(X)$ on the basis of the discussion in Ref. [57] for each pair of circumstances. Therefore, $P(X=1)$ and $P(X=0)$ are set to 0.5 in this verification framework.

^{*4} These are the extended datasets from those introduced in Ref. [58].

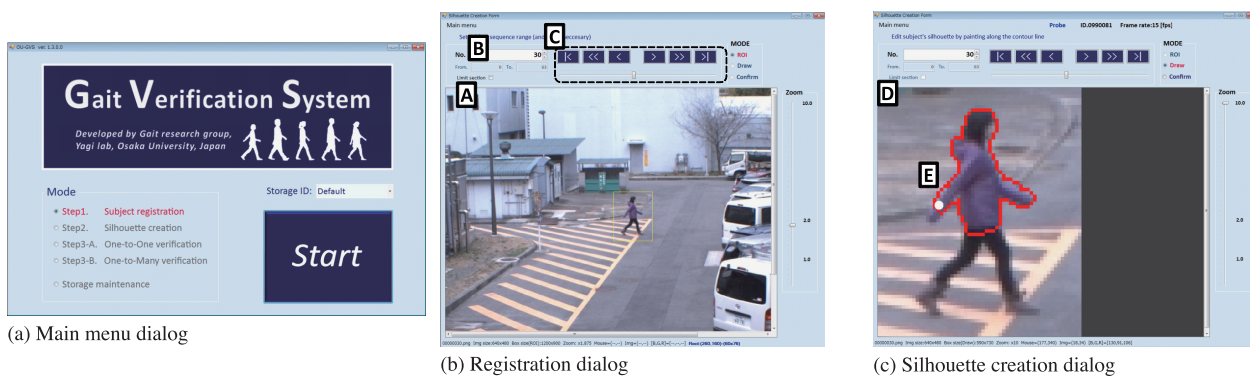


Fig. 5 Interface dialogs for the main menu, registration module, and silhouette creation module. (A) image in input sequence, (B) frame no. of the displayed image, (C) control panel for browsing image sequence, (D) cropped image of the subject, (E) subject's contour (red line) based on the silhouette created by the user.

Table 2 Typical functions and processing modes in each module.

Function	Processing mode
Registration module	
Image sequence input	Manual
Subject selection	Semi-automatic (interactive)
Subject registration	Manual
Silhouette creation module	
Silhouette creation	Semi-automatic (interactive)
Silhouette save	Manual
One-to-one/many verification module	
Feature extraction	Automatic
Feature masking	Manual
Probability calculation	Automatic

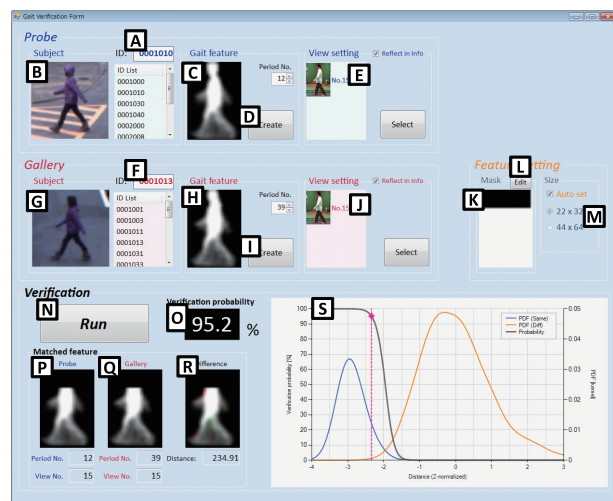


Fig. 6 Interface dialog for the one-to-one verification module. (A) ID of a selected probe subject, (B) cropped movie of the probe subject, (C) GEI of the probe subject, (D) button for the GEI creation of the probe subject, (E) observation view of the probe subject, (F) ID of a selected gallery subject, (G) cropped movie of the gallery subject, (H) GEI of the gallery subject, (I) button for GEI creation of the gallery subject, (J) observation view of the gallery subject, (K) mask region (black region corresponds to the mask), (L) button for opening the mask edit dialog shown in Fig. 11 (b), (M) size of the GEI, (N) run button for verification, (O) posterior probability, (P) probe GEI with mask (and view transformation), (Q) gallery GEI with mask (and view transformation), (R) image of the GEI difference, (S) PDFs of the current circumstances.

is summarized in Fig. 2, and typical functions for each module are listed in Table 2. Screenshot images of the interface dialogs for the four modules are shown in Fig. 5 (b) and (c), Fig. 6, and Fig. 7. These dialogs are started from a main menu dialog shown

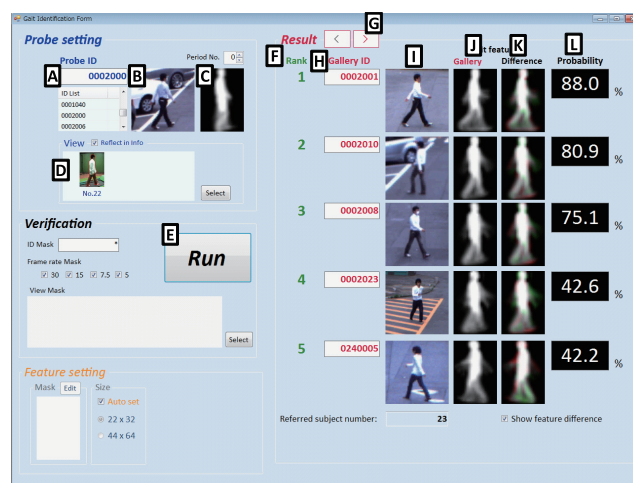


Fig. 7 Interface dialog for the one-to-many verification module. (A) ID of a selected probe subject, (B) cropped movie of the probe subject, (C) GEI of the probe subject, (D) observation view of the probe subject, (E) run button for verification, (F) ranking of posterior probabilities, (G) forward-reverse button of the rank list (rank 1 to 5 and rank 6 to 10), (H) IDs of the gallery subjects, (I) cropped movies of the gallery subjects, (J) GEIs of the gallery subjects, (K) images of the GEI difference, (L) posterior probabilities.

in Fig. 5 (a).

4.2 Processing Modes of Functions

As mentioned in Section 1, each step in the verification procedure for criminal investigation should be checked and judged by the user, because the verification result is required to have sufficient validity as criminal evidence. In addition, in some cases, manual operations are essential or more effective than automatic operations. For example, in the presence of multiple subjects in a footage, a target subject (e.g., perpetrator, suspect), can be specified only by a user (criminal investigator) who knows which is the target. Besides, in the case of the de-noising process in silhouette creation, interactive de-noising is often more effective than full-automatic de-noising. That is, if the user can manually specifies the noise region as a region of interest (ROI), the automatic de-noising process does not have to be applied to a whole image, but just applied to the ROI without affecting the remaining region of the image.

Consequently, we carefully set the processing modes for each



Fig. 9 View selection dialog. From these displayed views, a user selects the most similar view to the input view.

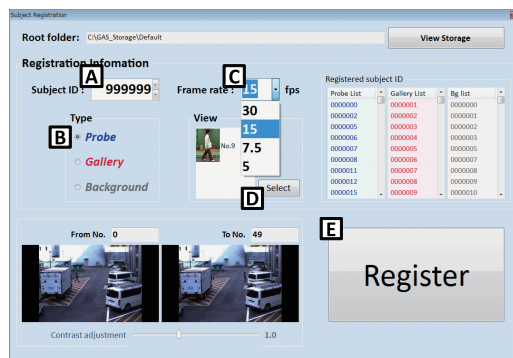


Fig. 8 Input dialog of the subject's information for registration. (A) ID, (B) subject's type, (C) frame rate, (D) button for opening the view selection dialog shown in Fig. 9, (E) run button for registration.

function in terms of system usability, efficiency, and validity: automatic, semi-automatic (interactive), and manual, as shown in Table 2.

4.3 User-system Interaction

This section briefly describes how a user interacts with the constructed system to complete the gait verification.

4.3.1 Registration Module

In this module, a user registers a target subject in the system. First, a user inputs the image sequence including a target subject and the first image of the sequence is displayed on the dialog as shown in Fig. 5 (A). The user then sets a section of the normal walking (stable walking interval) of the subject and a bounding box in each frame of the section. In the setting of a normal walking section, the user specifies the first and the last frames by visual checking. In the setting of the bounding boxes, the user sets the bounding boxes at the first and the last frames of the section manually (a rectangle drawing by mouse), and the bounding boxes at the remaining frames can then be set by an automatic interpolation function.

The user then registers the selected subject in the subject's database with information of the ID, type (probe, gallery or background^{*5}), captured frame rate, and observation view. An input dialog of this information is shown in Fig. 8. Note that the frame

^{*5} Typically, the type of *background* is the image sequence including no moving object and is used for silhouette creation.

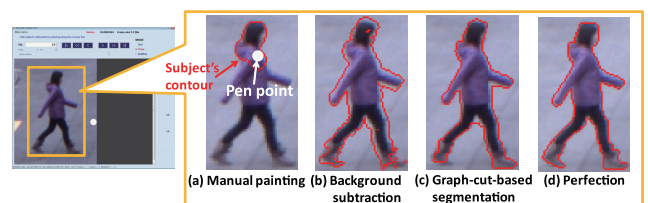


Fig. 10 Examples of the processing results on the silhouette creation dialog. (a) result of manual painting, (b) result of background subtraction, (c) result of graph-cut-based segmentation, (d) perfect silhouette after finalizing by manual painting.

rate is selected from the candidates indicated in the combo box shown in Fig. 8 (C), and the observation view is specified by selecting the most similar view to the input view from a view selection dialog^{*6} shown in Fig. 9, which is opened from a button shown in Fig. 8 (D).

4.3.2 Silhouette Creation Module

In this module, a user creates a silhouette sequence of the registered subject. First, a user selects a registered subject from the subject's database, and the subject's cropped image (the cropped region is based on the bounding box set in the registration module) is displayed on the dialog as shown in Fig. 5 (D). In this module, the subject's silhouette is shown to the user as the subject's contour line (red line) overlaid on the corresponding original image as shown in Fig. 5 (E).

The user creates the subject's silhouette for each frame mainly by using the mouse-based manual painting function and automatic functions of background subtraction and graph-cut-based segmentation [59]. The example on processing the results of these functions is shown in Fig. 10 (a), (b), and (c). In addition, some overall automatic functions such as area filtering, dilation, and erosion functions support the silhouette creation. The user can interactively adjust some parameters for each function (e.g., threshold for background subtraction) via the parameter adjust dialog.

One useful routine is as follows. First, a user runs the background subtraction function and then executes the graph-cut-based segmentation using the background subtraction results as the subject's seed region. Finally, the user checks all the silhou-

^{*6} Technically, an automatic view estimation is possible if the camera is correctly calibrated. However, the calibration requires specialist knowledge and hence it is almost impossible for users we assumed. For more details, see the discussion in Section 6.

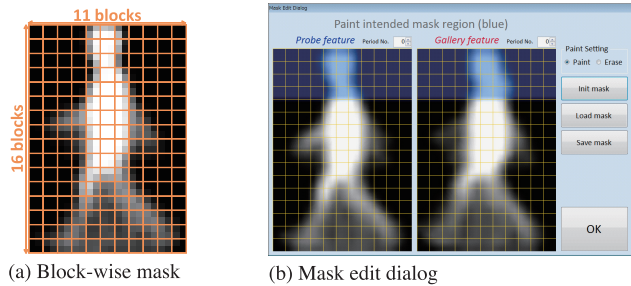


Fig. 11 Definition of block-wise mask and a dialog for feature mask specification. The block resolution is set to 11 by 16 blocks. In (b), the compared GEIs are displayed (probe on the left, gallery on the right) on the dialog and the translucent blue blocks indicate the user specified blocks as the mask.

ettes visually and modifies them using the manual painting function if necessary. An example of a perfect silhouette created by the above routine is shown in Fig. 10 (d).

After creating the subject's silhouettes, the user saves them to the subject's database.

4.3.3 One-to-one Verification Module

In this module, a user executes the one-to-one verification between the probe and gallery subjects registered in the system. First, the user selects a pair of registered probe and gallery subjects to be verified from the subject's database. Next, the user creates the GEI for each subject by pushing the button shown in Fig. 6 (D) and (I). The size of the GEI is automatically decided based on the smaller silhouette height of one of the two subjects so that the height of the GEI is smaller than the silhouette height (e.g., when the smaller silhouette height is 50 pixels, the size of the GEI is set as 22 by 32 pixels), and the size decided on is displayed on the dialog as shown in Fig. 6 (M).

The user then checks the outliers (differences in clothing or baggage conditions, such as wearing a helmet, hood, or backpack) in the compared GEIs and manually specifies such regions as mask regions if necessary. The mask region is set on the mask edit dialog shown in Fig. 11 (b), which is opened from a button shown in Fig. 6 (L). The mask blocks are specified by selecting the blocks displayed on the mask edit dialog as shown in Fig. 11 (b). Finally, a posterior probability of Eq. (3) is calculated and the result is displayed on the dialog as shown in Fig. 6 (O).

4.3.4 One-to-many Verification Module

In this module, a user executes the one-to-many verification between probe and gallery subjects registered in the system. First, the user selects a subject to be verified from a probe list of the subject's database. The user then verifies the subject against all the gallery subjects in the subjects' database by pushing the button shown in Fig. 7 (E), and the verification results are displayed on the dialog in the form of a list of gallery subjects, in which the top ten subjects with higher posterior probabilities are sorted in descending order as shown in Fig. 6 (L).

4.4 Implementation

The system was implemented on the mixed platform of C#, C++/CLI, and C++ using Visual Studio 2008 (Professional Edition) with .net framework 3.5 SP1. The OpenCV library (version 2.3) was also used for image processing. The system runs on

computers operating Windows XP, Windows Vista, or Windows 7.

5. Experiment

In this experiment, we conducted the operation test of the constructed system with a total of eleven participants composed of a gait-specialist (who was also the implementer of the system) and ten non-gait-specialists with sufficient computer literacy (e.g., technical support staff and students in our laboratory at the University). The aim of this operation test was to confirm that the non-gait-specialists can use the system following a brief instruction manual, and more specifically, they, as well as the gait-specialist, can obtain reasonable results in a reasonable time on their own. We tested this with the one-to-one verification scenario^{*7}.

5.1 Instruction to the Participants

First, all the non-gait-specialists received a 90-minute instruction on the outline of gait verification and how to use the system with a manual. They then practiced the operation of the system for 3 to 5 hours using preliminary datasets for verification, while receiving advice from the system implementer.

5.2 Test Datasets

Five verification datasets were arranged for the operation test. Sample images of each dataset are shown in Table 3 and the details of each dataset are shown in Table 4. Note that the build and height of each gallery subject are similar to those of the other gallery subjects in the same dataset, and hence each dataset is challenging in terms of verification.

5.3 Test Results

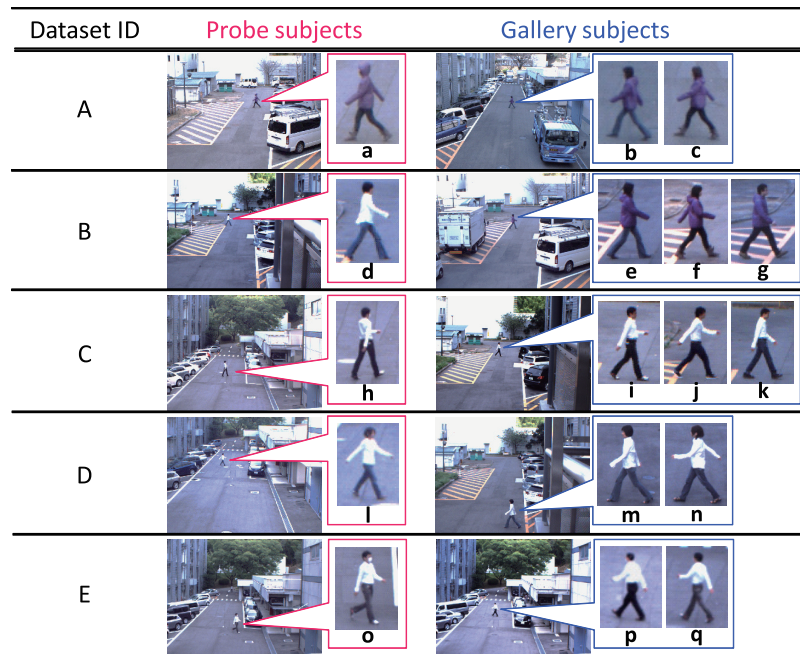
The verification outputs (posterior probabilities) for the 11 participants are summarized in Table 5, and the operation times (average, minimum, and maximum) in each module are summarized in Table 6. Note that the column for "ground truth" indicates that a pair of probe and gallery subjects are either the same or different subjects in Table 5, and that participant #1 is the gait-specialist, while the others are the non-gait-specialists in both tables. Note that the gait-specialist obtained reasonable results for all the datasets, namely, the posterior probabilities for pairs for the same subjects are extremely high (more than 89.9%) while those for the pairs of different subjects are low (less than 35.4%).

5.3.1 Verification Outputs

First, we focused on the clothing variations of datasets A and B. For dataset A, the probe subject *a* wore a hood while the gallery subjects *b* and *c* did not. Therefore, the associated parts had to be masked to obtain a valid result. For this set, all the participants successfully masked the head region and as a result, the results for all the participants show the same tendency in Table 5.

In addition, for dataset B, whereas the probe subject *d* wore tight outer clothing, the gallery subjects *e*, *f*, and *g* wore loose

^{*7} In terms of user operation, operations of the one-to-many verification module are almost the same as the one-to-one verification module. Therefore, we conducted the operation test using only the one-to-one verification scenario.

Table 3 Sample images of the datasets for the operation test.**Table 4** Details of the datasets for the operation test.

Dataset ID	Subject ID	Subjects' height (approx.) [pixel]	Number of images in a section normal walking (approx.)	Frame rate [fps]	View
A	a	60	70	15	Left lateral
	b	50	65	15	Left lateral
	c	50	70	15	Left lateral
B	d	80	40	7.5	Right lateral
	e	95	30	7.5	Right lateral
	f	95	35	7.5	Right lateral
	g	95	30	7.5	Right lateral
C	h	65–75	90	15	Right rear oblique
	i	90	65	15	Right lateral
	j	90	60	15	Right lateral
	k	90	80	15	Right lateral
D	l	50–55	60	15	Right front oblique
	m	120	50	15	Left lateral
	n	120	50	15	Left lateral
E	o	85–98	55	7.5	Right front oblique
	p	55–60	55	15	Left rear oblique
	q	55–60	60	15	Left rear oblique

outer clothes with hoods. Hence the associated upper body parts needed to be masked. For this set, while nine participants successfully masked the associated upper body parts, the other two participants (#6 and #9) masked only the hooded parts. As a result, the posterior probabilities for the same subject pairing by the two participants were slightly lower than those for the other participants as shown in Table 5. In fact, the results were actually improved by retrying masking the upper part of both participants. More specifically, the posterior probabilities of participants #6 and #9 for the same subject pairing were changed from 76.7% to 85.1% and from 87.0% to 95.4%, while those for the different subject pairings were changed from 0.3% to 1.6% (subject f) and from 0.0% to 0.0% (subject g), and from 1.7% to 11.3% (subject f) and from 0.0% to 0.0% (subject g).

Next, we focused on the view variations of datasets C, D, and E. In Table 5, we see that the results for datasets C and E obtained by all the participants indicate the same tendency. In fact, for these datasets, all the participants appropriately selected the

observation views of the probe and gallery subjects.

Conversely, for dataset D, two participants (#6 and #9) mis-selected observation views (tilt types) of the gallery subjects^{*8}, because they did not have a firm understanding of observation view, in particular, the tilt view. This mis-selection decreased the validity of the verification, particularly in terms of view transformation. Consequently, the posterior probabilities obtained by #6 and #9 declined compared to those of the other participants as shown in Table 5.

Note that, after receiving additional training lectures w.r.t. observation views, the two participants #6 and #9 were able to select the appropriate view, and the results were improved: the posterior probabilities of participants #6 and #9 for the same subject pairing were changed from 46.0% to 84.8% and from 65.9% to 89.5%, while those for the different subject pairings were changed from 22.3% to 58.2% and from 25.9% to 51.5%.

^{*8} In dataset D, while the appropriate view is camera 15 in Fig. 9 with almost no tilt, the selected view was camera 11 in Fig. 9 with tilt.

Table 5 Verification outputs (posterior probabilities) of each participant [%].

Dataset ID	Subject ID		Ground truth	Participant ID										
	Probe	Gallery		1	2	3	4	5	6	7	8	9	10	11
A	a	b	Different	0.4	20.5	4.3	0.2	4.2	0.5	0.9	0.7	2.2	0.9	1.6
		c	Same	95.2	90.2	96.7	93.4	80.4	83.4	97.3	97.6	89.4	94.5	99.5
B	d	e	Same	96.0	96.7	95.1	97.7	92.7	76.7	96.5	88.4	87.0	96.7	93.0
		f	Different	11.0	30.0	10.6	18.0	4.0	0.3	23.7	17.9	1.7	0.2	3.9
		g	Different	0.0	0.0	0.0	0.0	0.0	0.0	0.0	0.0	0.0	0.0	0.0
C	h	i	Same	89.9	89.4	89.1	77.6	90.5	90.5	83.9	83.6	86.5	90.0	88.6
		j	Different	3.8	7.7	15.3	3.9	7.7	4.9	3.8	5.7	4.4	4.8	3.3
		k	Different	7.9	8.8	13.4	8.0	11.7	14.0	11.6	7.5	11.2	8.4	12.3
D	l	m	Different	35.4	37.0	54.9	29.0	30.4	22.3	36.2	35.5	25.9	36.7	35.7
		n	Same	91.5	81.0	89.1	73.5	85.0	46.0	73.3	74.4	65.9	72.9	85.6
E	o	p	Different	32.5	33.5	29.1	39.5	27.1	31.4	34.6	30.3	33.4	30.5	30.5
		q	Same	93.3	88.1	89.8	86.6	88.3	80.4	87.3	91.1	74.5	87.5	88.9

Table 6 Approximate operation times for each participant [min].

Module		Participant ID											Average
		1	2	3	4	5	6	7	8	9	10	11	
Register	Average	2	4	4	5	4	3	4	4	5	4	4	4
	Min/Max	2/3	2/7	2/6	5/5	2/6	2/5	3/5	3/9	5/5	3/8	2/7	
Silhouette	Average	25	18	24	22	19	19	30	18	22	16	19	21
	Min/Max	5/42	7/37	9/46	10/45	6/35	10/30	13/48	7/30	10/40	5/38	6/33	
One-to-one verification	Average	1	1	1	1	2	1	2	2	2	1	1	1
	Min/Max	1/1	1/1	1/2	1/1	1/3	1/2	1/3	1/2	2/2	1/2	1/1	
Whole verification process	Average	59	49	62	59	51	46	74	46	59	45	50	
	Min/Max	36/82	33/77	35/85	41/76	27/82	32/59	47/100	27/58	37/82	24/77	29/76	

In total, all the non-gait-specialists obtained the results which indicated the same tendency with those of the gait-specialist for almost all the verification datasets (46 verification pairs out of 50). On the other hand, in addition to unsatisfactory results of participants #6 and #9 for dataset B and E (4 pairs as mentioned above), we notice that there still exist certain inter-user deviations of the posterior probabilities even if excluding the participants #6 and #9 (e.g., from 72.9% to 91.5% for dataset D). Therefore, these results imply that more practice is desirable in selecting the appropriate mask region and observation views for such failure participants and also further improvements to suppress the inter-user deviations of the posterior probability as discussed in Section 6.

5.3.2 Operation Times

Focusing on operation times in Table 6, these varied to some extent depending on the participants. The averaged working times for subject registration, silhouette creation, and one-to-one verification were 4 minutes, 21 minutes, and 1 minutes and a detailed breakdown is shown in Table 6. To carry out the whole verification process, it was necessary to use the registration and silhouette modules twice, and the verification module once. In these evaluation experiments, the whole verification process was completed in 24 minutes for the shortest case, and only 100 minutes for the longest case. These results show that each participant obtained the verification results within reasonable operation times.

6. Discussion

6.1 Inter-user Deviation in the Manual Operation

Although it was shown that reasonable results were provided by almost all the verification pairs in the experiments, there still remained certain deviations from expectation owing to inter-user variations in the manual operations such as the selection of image

sequence intervals, observation views, and feature masks. Therefore, it seems worthwhile to introduce semi-automatic functions to reduce these deviations.

One of the potential countermeasures exploits walking trajectories in selecting stable walking intervals and estimating the observation views automatically. Assuming a ground plane constraint for the calibrated camera, the walking trajectory is relatively easy to extract as a sequence of footprints on the ground plane [60], [61]. Although camera calibration is essential for this purpose, on-site camera calibration using calibration targets is a troublesome procedure, and almost impossible for the non-specialist. This is the main reason why our system does not contain a function for estimating walking trajectories.

Bazin et al. [62] proposed an alternative method for image-based camera calibration using vanishing points estimated from lines in a scene (e.g., buildings, roads, corridors), although the method has an intrinsic ambiguity w.r.t. scale. It is, however, still useful in estimating walking trajectories because scale information is not needed just to select stable walking intervals and to estimate observation views. Thus, the automatically-selected walking intervals and estimated observation views are shown to a user as candidates, and these are manually modified by the user if necessary. These are indeed semi-automatic functions.

As for gait feature masking, there are several potential approaches for inferring regions to be masked (e.g., masked GEI [3], clothing change-aware part-based gait recognition [56], backpack detection [63], and carried-item detection [64]). Therefore, such automatically inferred regions can be shown to a user for possible masking, and manually modified by the user if necessary, which is also a semi-automatic function.

In this way, it is expected that semi-automatic functions would reduce the deviation between users and that more stable posterior probabilities would be provided.

6.2 Improvement of the VTM

Although the VTM implemented in our system basically works well, the performance for cross-view matching is still worse than for same-view matching. In fact, whereas an averaged posterior for the same subjects in the same-view matching (pairs of probe a and gallery c , probe d and gallery e) is 94.3%, while that in cross-view matching (pairs of probe h and gallery i , probe l and gallery n , probe o and gallery q) is 85.7%^{*9}. Nevertheless, it has been reported that the accuracy of VTM can be improved by using multi-view references in Refs. [2] and [65], and hence the performance of cross-view matching can be improved with the additional effort of collecting more footage from different views of suspect targets.

Degradation in the performance for cross-view matching can also be caused by view differences between the actual probe/gallery view and the user-selected view from the 24 discrete views shown in Fig. 9. One effective countermeasure for this problem is to introduce an arbitrary view transformation model [66], where gait data of non-target training subject (e.g., volunteers such as lab. members) are stored as exemplar in the form of a 3D gait volume sequence. Using the 3D gait volume sequences of non-target training subjects, we can obtain 2D gait silhouettes of the non-target subjects projected to arbitrary views of target subjects (e.g., perpetrator and suspect). Thereafter, the discrete VTM used in this paper is applicable in the same way.

Thus, there is further room for improvement in cross-view matching by taking the above two points into consideration in the future.

7. Conclusion

We constructed the first gait verification system for criminal investigation. The system was designed so that criminal investigators as non-gait-specialists could obtain without assistance vision-based gait verification results between perpetrators and suspects. The system outputs verification results between compared subjects in the form of the posterior probability that indicates whether they are the same subjects, considering circumstances such as the subject size, frame rate, clothing, and observation views. We conducted an operation test of the constructed system with one gait-specialist and ten non-gait-specialists. All the non-gait-specialists, as well as the gait-specialist, obtained reasonable verification results for almost all the verification sets.

Although there is still room for improvement in system usability and accuracy of verification, we believe that this system will allow criminal investigators to use gait verification, which will contribute much to more efficient criminal investigation. A seminar of the constructed system for Japanese police is planned in the near future.

Acknowledgments This work was partly supported by JSPS Grant-in-Aid for Scientific Research(S) 21220003 and “R&D Program for Implementation of Anti-Crime and Anti-Terrorism Technologies for a Safe and Secure Society”, Strategic Funds for the Promotion of Science and Technology of the Ministry of Education, Culture, Sports, Science and Technology, the Japanese

Government.

References

- [1] Han, J. and Bhanu, B.: Individual Recognition Using Gait Energy Image, *Trans. Pattern Analysis and Machine Intelligence*, Vol.28, No.2, pp.316–322 (2006).
- [2] Makiyara, Y., Sagawa, R., Mukaigawa, Y., Echigo, T. and Yagi, Y.: Gait Recognition Using a View Transformation Model in the Frequency Domain, *Proc. 9th European Conf. Computer Vision*, Graz, Austria, pp.151–163 (2006).
- [3] Bashir, K., Xiang, T. and Gong, S.: Gait recognition without subject cooperation, *Pattern Recogn. Lett.*, Vol.31, No.13, pp.2052–2060 (2010).
- [4] Lam, T.H.W., Cheung, K.H. and Liu, J.N.K.: Gait flow image: A silhouette-based gait representation for human identification, *Pattern Recogn.*, Vol.44, pp.973–987 (2011).
- [5] Wang, C., Zhang, J., Wang, L., Pu, J. and Yuan, X.: Human Identification Using Temporal Information Preserving Gait Template, *IEEE Trans. Pattern Analysis and Machine Intelligence*, Vol.34, No.11, pp.2164–2176 (2012).
- [6] How biometrics could change security, BBC (online), available from http://news.bbc.co.uk/2/hi/programmes/click_online/7702065.stm (accessed 2013-01-25).
- [7] Bouchrika, I., Goffredo, M., Carter, J. and Nixon, M.: On Using Gait in Forensic Biometrics, *Journal of Forensic Science*, Vol.56, No.4, pp.882–889 (2011).
- [8] Nixon, M.S. and Carter, J.N.: Automatic recognition by gait, *Proc. IEEE*, Vol.94, No.11, pp.2013–2024 (2006).
- [9] Iwama, H., Okumura, M., Makiyara, Y. and Yagi, Y.: The OU-ISIR Gait Database Comprising the Large Population Dataset and Performance Evaluation of Gait Recognition, *IEEE Trans. Information Forensics and Security*, Vol.7, No.5, pp.1511–1521 (2012).
- [10] Utsumi, A. and Tetsutani, N.: Adaptation of appearance model for human tracking using geometrical pixel value distributions, *Proc. 6th Asian Conf. Computer Vision*, Vol.2, pp.794–799 (2004).
- [11] Yu, S., Tan, D. and Tan, T.: Modelling the Effect of View Angle Variation on Appearance-Based Gait Recognition, *Proc. 7th Asian Conf. Computer Vision*, Vol.1, pp.807–816 (2006).
- [12] Akae, N., Mansur, A., Makiyara, Y. and Yagi, Y.: Video from nearly still: An application to low frame-rate gait recognition, *Proc. IEEE Computer Society Conf. Computer Vision and Pattern Recognition 2012*, Vol.1, pp.1537–1543 (2012).
- [13] Iwama, H., Muramatsu, D., Makiyara, Y. and Yagi, Y.: Gait-based Person-Verification System for Forensics, *Proc. 5th IEEE Int. Conf. Biometrics: Theory, Applications and Systems*, Washington D.C., USA, pp.1–8 (2012).
- [14] Lu, J. and Tan, Y.-P.: Gait-Based Human Age Estimation, *IEEE Trans. Information Forensics and Security*, Vol.5, No.4, pp.761–770 (2010).
- [15] Makiyara, Y., Okumura, M., Iwama, H. and Yagi, Y.: Gait-based Age Estimation using a Whole-generation Gait Database, *Proc. International Joint Conference on Biometrics (IJCB2011)*, Washington D.C., pp.1–6 (2011).
- [16] Yu, S., Tan, T., Huang, K., Jia, K. and Wu, X.: A study on gait-based gender classification, *IEEE Trans. Image Processing*, Vol.18, No.8, pp.1905–1910 (2009).
- [17] Bobick, A. and Johnson, A.: Gait Recognition using Static Activity-specific Parameters, *Proc. IEEE Conf. Computer Vision and Pattern Recognition*, Vol.1, pp.423–430 (2001).
- [18] Yam, C., Nixon, M. and Carter, J.: Automated Person Recognition by Walking and Running via Model-based Approaches, *Pattern Recogn.*, Vol.37, No.5, pp.1057–1072 (2004).
- [19] Yang, H.-D. and Lee, S.-W.: Reconstruction of 3D human Body Pose for Gait Recognition, *Proc. IAPR Int. Conf. Biometrics 2006*, pp.619–625 (2006).
- [20] Ariyanto, G. and Nixon, M.: Marionette mass-spring model for 3D gait biometrics, *Proc. 5th IAPR Int. Conf. Biometrics*, pp.354–359 (2012).
- [21] Liu, Z. and Sarkar, S.: Simplest Representation Yet for Gait Recognition: Averaged Silhouette, *Proc. 17th Int. Conf. Pattern Recognition*, Vol.1, pp.211–214 (2004).
- [22] Sarkar, S., Phillips, J., Liu, Z., Vega, I., Ther, P.G. and Bowyer, K.: The HumanID Gait Challenge Problem: Data Sets, Performance, and Analysis, *Trans. Pattern Analysis and Machine Intelligence*, Vol.27, No.2, pp.162–177 (2005).
- [23] DUI Gait Analysis Defense — Forensic DUI Defense, available from <http://duigait.com/work.html> (accessed 2013-01-25).
- [24] Gait Analysis — Identification of persons by the style and features of their walk, available from <http://www.gaitforensic.com> (accessed 2013-01-25).

^{*9} In the calculation of the average score, the scores of participants #6 and #9 are excluded because of their mis-operations described in Section 5.3.

- [25] Forensic Gait Analysis, available from (<http://www.podia-clinic.com/forensic/>) (accessed 2013-01-25).
- [26] The OU-ISIR Gait Database, Large Population Dataset, Osaka University (online), available from (<http://www.am.sanken.osaka-u.ac.jp/BiometricDB/GaitLP.html>) (accessed 2013-02-01).
- [27] Matovski, D., Nixon, M.S., Mahmoodi, S. and Carter, J.: The Effect of Time on Gait Recognition Performance, *IEEE Trans. Information Forensics and Security*, Vol.7, No.2, pp.543–552 (2012).
- [28] Bruegge, R.V.: Biometrics and Forensics: Similarities and Differences, *Biometric Consortium 2004 Conference* (2004).
- [29] Dessimoz, D. and Champod, C.: Linkages between Biometrics and Forensic Science, *Handbook of Biometrics*, Jain, A.K., Flynn, P. and Ross, A.A. (Eds.), chapter 19, pp.425–459, Springer Science+Business Media, LLC (2008).
- [30] Bertillon, A.: *Identification Anthropometrique et Instructions Signaletiques*, Imprimerie Administrative, Melun (1893).
- [31] Faulds, H.: On the skin-furrows on the hands, *Nature*, Vol.22, p.605 (1880).
- [32] Hershel, W.: Skin furrows on the hand, *Nature*, Vol.23, p.76 (1880).
- [33] Galton, F.: Method of indexing Fingermarks, *Nature*, Vol.44, p.141 (1891).
- [34] Henry, E.: *Classification and Uses of Finger Prints*, George Routledge and Sons (1900).
- [35] Komarinski, P.: *Automated fingerprint identification systems (AFIS)*, Academic Press (2005).
- [36] Butler, J.M.: *Forensic DNA typing*, Elsevier Academic Press (2005).
- [37] de Jong, W., van der Kooij, L.K. and Schmidt, D.: Computer aided analysis of handwriting, the NIFO-TNO approach, *Proc. 4th European Handwriting Conference for Police and Government Handwriting Experts* (1994).
- [38] Franke, K. and Köppen, M.: A computer-based system to support forensic studies on handwritten documents, *IJDAR*, Vol.3, No.4, pp.218–231 (2001).
- [39] Franke, K., Schomaker, L., Veenhuis, C., Taubenheim, C., Guyon, I., Vuurpijl, L., van Erp, M. and Zwarts, G.: WANDA: A generic Framework applied in Forensic Handwriting Analysis and Writer Identification, *HIS*, pp.927–938 (2003).
- [40] Champod, C., Evett, I.W. and Kuchler, B.: Earmarks as Evidence: A Critical Review, *Journal of Forensic science*, Vol.46, No.6, pp.1275–1284 (2001).
- [41] Alberink, I. and Ruifrok, A.: Performance of the FearID earprint identification system, *Forensic Science International*, Vol.166, pp.145–54 (2007).
- [42] Pretty, I.A. and Sweet, D.: A look at forensic dentistry - Part 1: The role of teeth in the determination of human identity, *British Dental Journal*, Vol.190, pp.359–366 (2001).
- [43] Adams, B.: The diversity of adult dental patterns in the United States and the implications for personal identification, *Journal of Forensic Science*, Vol.48, No.3, pp.497–503 (2003).
- [44] Champod, C. and Muewly, D.: The inference of identity in forensic speaker recognition, *Speech Communication*, Vol.31, pp.193–203 (2000).
- [45] Rose, P.: *Forensic Speaker Identification*, CRC Press (2002).
- [46] Neustein, A. and Patil, H.A. (Eds.): *Forensic Speaker Recognition Law Enforcement and Counter-Terrorism*, Springer Science+Business Media, LLC (2012).
- [47] Iscan, M.Y.: Introduction of techniques for photographic comparison: Potential and problems, *Forensic Analysis of the Skull: Craniofacial Analysis, Reconstruction, and Identification*, pp.57–70, Wiley-Liss (1993).
- [48] Vanezis, P. and Brierley, C.: Facial Image Comparison of Crime Suspects Using Video Superimposition, *Science & Justice*, Vol.36, No.1, pp.27–33 (1996).
- [49] Vanezis, P., Lu, D., Cockburn, J., Gonzalez, A., McCombe, G., Trujillo, O. and Vanezis, M.: Morphological classification of facial features in adult Caucasian males based on an assessment of photographs of 50 subjects, *Journal of Forensic Sciences*, Vol.41, No.5, pp.786–791 (1996).
- [50] Yoshino, M.: Conventional and novel methods for facial-image identification, *Forensic Science Review*, Vol.16, No.2, pp.104–114 (2004).
- [51] Lynnerup, N. and Vedel, J.: Person Identification by Gait Analysis and Photogrammetry, *Journal of Forensic science*, Vol.50, No.1, pp.112–118 (2005).
- [52] Larsen, P.K., Simonsen, E.B. and Lynnerup, N.: Gait Analysis in Forensic Medicine, *Journal of Forensic Sciences*, Vol.53, No.5, pp.1149–1153 (online), DOI: 10.1111/j.1556-4029.2008.00807.x (2008).
- [53] FaceIt® Argus - Solutions - L-1 Identity Solutions, available from (<http://www.11id.com/pages/71-faceit-argus>) (accessed 2013-01-28).
- [54] Moreno, A. and Grigoros, C.: Automatic Speaker Recognition Methodology Using BATVOX, *Symposium of Forensic Sciences* (2007).
- [55] Alese, B.K., Mogaji, S., Adewale, O.S. and Daramola, O.: Design and Implementation of Gait Recognition System, *International Journal of Engineering and Technology*, Vol.2, No.7, pp.1102–1110 (2012).
- [56] Hossain, M.A., Makiyara, Y., Wang, J. and Yagi, Y.: Clothing-Invariant Gait Identification using Part-based Clothing Categorization and Adaptive Weight Control, *Pattern Recognition*, Vol.43, No.6, pp.2281–2291 (2010).
- [57] Hummel, K.: On the Theory and Practice of Essen-Möller's W value and Gürtler's Paternity Index (PI), *Forensic Science International*, Vol.25, pp.1–17 (1984).
- [58] Makiyara, Y., Mannami, H., Tsuji, A., Hossain, M., Sugiura, K., Mori, A. and Yagi, Y.: The OU-ISIR Gait Database Comprising the Treadmill Dataset, *IPJS Trans. Computer Vision and Applications*, Vol.4, pp.53–62 (2012).
- [59] Boykov, Y. and Jolly, M.: Interactive graph cuts for optimal boundary and region segmentation of objects in n-d images, *Proc. Int. Conf. Computer Vision*, Vol.1, pp.105–112 (2001).
- [60] Hild, M.: Estimation of 3D Motion Trajectory and Velocity from Monocular Image Sequences in the Context of Human Gait Recognition, *Proc. 17th Int. Conf. Pattern Recognition*, Vol.1, pp.231–235 (2004).
- [61] Makiyara, Y., Sagawa, R., Mukaigawa, Y., Echigo, T. and Yagi, Y.: Adaptation to Walking Direction Changes for Gait Identification, *Proc. 18th Int. Conf. Pattern Recognition*, Vol.2, Hong Kong, China, pp.96–99 (2006).
- [62] Bazin, J.-C., Seo, Y., Demonceaux, C., Vasseur, P., Ikeuchi, K., Kweon, I. and Pollefeys, M.: Globally Optimal Line Clustering and Vanishing Point Estimation in Manhattan World, *Proc. 25th IEEE Conf. Computer Vision and Pattern Recognition*, pp.638–645 (2012).
- [63] Decann, B. and Ross, A.: Gait curves for human recognition, backpack detection, and silhouette correction in a nighttime environment, *Proc. SPIE, Biometric Technology for Human Identification VII*, Vol.7667, pp.76670Q–76670Q–13 (2010).
- [64] Damen, D. and Hogg, D.: Detecting Carried Objects from Sequences of Walking Pedestrians, *IEEE Trans. Pattern Analysis and Machine Intelligence*, Vol.34, No.6, pp.1056–1067 (2012).
- [65] Kusanniran, W., Wu, Q., Zhang, J. and Li, H.: Support Vector Regression for Multi-View Gait Recognition based on Local Motion Feature Selection, *Proc. IEEE Computer Society Conf. Computer Vision and Pattern Recognition 2010*, San Francisco, CA, USA, pp.1–8 (2010).
- [66] Muramatsu, D., Shiraishi, A., Makiyara, Y. and Yagi, Y.: Arbitrary View Transformation Model for Gait Person Authentication, *Proc. 5th IEEE Int. Conf. Biometrics: Theory, Applications and Systems*, No. Paper ID 39, Washington D.C., USA, pp.1–6 (2012).



Haruyuki Iwama received his B.S. and M.S. degrees in Engineering and Ph.D. in Information Science from Osaka University in 2003, 2005, and 2012, respectively. In 2005, he joined the Production Technology Development Group, Sharp Corporation, where he worked on vision-based inspection systems. He is currently

a Specially Appointed Researcher of the Institute of Scientific and Industrial Research, Osaka University. His research interests are multi-view shadow and foreground segmentation, group context-based person identification, and gait recognition.



Daigo Muramatsu received his B.S., M.E., and Ph.D. degrees in Electrical, Electronics, and Computer Engineering from Waseda University in 1997, 1999, and 2006, respectively. He is currently a Specially Appointed Associate Professor of the Institute of Scientific and Industrial Research, Osaka University. His

research interests are gait recognition, signature verification, and biometric fusion. He is a member of IEEE, IEICE, and IIEEJ.



Yasushi Makihara received his B.S., M.S., and Ph.D. degrees in Engineering from Osaka University in 2001, 2002, and 2005, respectively. He is currently an Assistant Professor of the Institute of Scientific and Industrial Research, Osaka University. His research interests are

gait recognition, morphing, and temporal super resolution. He is a member of IPSJ, RJS, and JSME.



Yasushi Yagi is the Director of the Institute of Scientific and Industrial Research, Osaka university, Ibaraki, Japan. He received his Ph.D. degrees from Osaka University in 1991. In 1985, he joined the Product Development Laboratory, Mitsubishi Electric Corporation, where he worked on robotics and in-

spection. He became a Research Associate in 1990, a Lecturer in 1993, an Associate Professor in 1996, and a Professor in 2003 at Osaka University. International conferences for which he has served as Chair include: FG1998 (Financial Chair), OMINVIS2003 (Organizing chair), ROBIO2006 (Program co-chair), ACCV2007 (Program chair), PSVIT2009 (Financial chair), ICRA2009 (Technical Visit Chair), ACCV2009 (General chair), ACPR2011 (Program co-chair) and ACPR2013 (General chair). He has also served as the Editor of IEEE ICRA Conference Editorial Board (2007–2011). He is the Editorial member of IJCV and the Editor-in-Chief of IPSJ Transactions on Computer Vision & Applications. He was awarded ACM VRST2003 Honorable Mention Award, IEEE ROBIO2006 Finalist of T.J. Tan Best Paper in Robotics, IEEE ICRA2008 Finalist for Best Vision Paper, MIRU2008 Nagao Award, and PSIVT2010 Best Paper Award. His research interests are computer vision, medical engineering and robotics. He is a fellow of IPSJ and a member of IEICE, RSJ, and IEEE.

(Communicated by *Greg Mori*)